Dyes and Pigments 148 (2018) 236–248

Contents lists available at ScienceDirect

Dyes and Pigments

journal homepage: www.elsevier.com/locate/dyepig

Pigment-binder interactions in calcium-based tempera paints

Kerstin Elert*, Agustin Herrera, Carolina Cardell

Department of Mineralogy and Petrology, Faculty of Science, University of Granada, Avenida Fuentenueva s/n, 18071 Granada, Spain

ARTICLE INFO

Article history:
Received 31 July 2017
Received in revised form
1 September 2017
Accepted 8 September 2017
Available online 11 September 2017

Keywords:
Calcite
Portlandite
Vaterite
Bianco di San Giovanni
Rabbit glue
Aging tests

ABSTRACT

Calcium hydroxide and calcium carbonate, or mixtures of both have been used for millennia as pigments or primers, often in combination with proteinaceous binders. Despite their historical importance and widespread use in wall paintings, little research has been dedicated to possible interactions between the inorganic pigment and the organic binder, and their impact on paint aging under variable environmental conditions. Here, paint dosimeters mimicking historic paints were exposed to artificial UV-aging and long-term outdoor exposure tests and analyzed using a wide array of techniques, including x-ray diffraction, scanning electron microscopy, attenuated total reflectance-Fourier transform infrared spectroscopy, thermogravimetry, laser particle size analysis, and spectrophotometry. Our results show that the prevailing environmental conditions (i.e., sheltered or directly exposed to rain and sunlight) and the presence or absence of proteinaceous binder have a significant influence on the mineralogical and morphological evolution of paints containing calcium hydroxide. The organic binder delays carbonation and induces the formation of hybrid materials similar to biominerals, incorporating organics into the inorganic carbonate matrix. Such a biomimetic effect significantly enhances the durability of the paint layer. Calcium carbonate pigments, in contrast, did not suffer mineralogical changes in the presence of organic binder. However, both, calcium carbonate and hydroxide caused conformational changes in the proteinaceous binder. Observed differences in pigment-binder interactions have an important influence on the paints' resistance to chemical weathering, explain different alteration patterns observed in historic paints under semi-open exposure conditions, and allow for recommendations regarding the most suitable material for wall painting conservation considering the prevailing environmental conditions.

1. Introduction

Throughout history calcium carbonate has been extensively used as a painting material, either as a pigment, often as an extender blended with more expensive white pigments, or as a primer [1]. The pigment can be made of ground limestone (marble) or chalk [2]. It shows good hiding power in water-based systems (i.e., tempera paints with egg yolk, casein, or rabbit glue binder) and is often mixed with animal glue when used as a primer. Early examples of its use as a pigment include the Lascaux and Roucadour cave paintings from the Palaeolithic period [3]. Apart from pure calcium carbonate, "Bianco di San Giovanni" (BSG) a white pigment made of partially carbonated lime has been used in fresco and tempera paintings. This pigment was first mentioned by Cennino Cennini in his "Il Libro dell Arte", but was most likely used before Cennini's time [4,5]. According to Colalucci [6] Michelangelo used this pigment as a base for certain reds and yellows in the frescoes of the Sistine Chapel. Slaked lime ($Ca(OH)_2$) was also used as binding media for pigments applied in wall paintings (fresco technique). Earliest examples are found in Greece and Italy [1].

Despite their historical importance and widespread use as painting materials, little research has been dedicated to the interaction of calcium-based pigments and proteinaceous binders [2,5,7–9]. High pH, especially in the case of calcium hydroxide (pH = 12.5), might cause changes in the structure of proteins and will consequently affect the paint's stability over time [10].

Up to now, no detailed studies are available which would clarify this aspect. Furthermore, the calcium hydroxide in BSG-based paints inevitably carbonates once applied and exposed to ambient air and mineralogical and morphological changes that can alter the paints' properties will occur.

Here we examined the effect of different calcium-based pigments (pure calcium carbonate or calcium hydroxide, and mixtures of both) on conformational changes in rabbit glue used as organic binder. We also tracked the morphological changes of calcium-

* Corresponding author.
E-mail address: kelert@ugr.es (K. Elert).

http://dx.doi.org/10.1016/j.dyepig.2017.09.013
0143-7208/

based pigments with or without organic binder under UV-aging conditions. Besides laboratory tests, paint dosimeters prepared following historic recipes, were placed over a period of 30 months in strategic locations in the city of Granada, Spain (i.e., the historic city center and the Alhambra monument), and textural, mineralogical, morphological, and conformational changes were examined using a wide range of analytical techniques, including x-ray diffraction (XRD), scanning electron microscopy (SEM), attenuated total reflectance-Fourier transform infrared spectroscopy (ATR-FTIR), thermogravimetry (TG), laser particle size analysis, and spectrophotometry. Our ultimate goal was to further the current knowledge on pigment-binder interactions in order to help explain observed alteration patterns in historic paintings, and assist in the selection of appropriate conservation materials for wall paintings, especially those suffering *T* and relative humidity (RH) fluctuations in semi-open courtyards or halls.

2. Materials and methods

2.1. Materials

Pigments and rabbit glue were purchased from Kremer Pigmente GmbH & Co, Germany. The pigments and binder include "Bianco di San Giovanni" standard (No.11415), "Bianco di San Giovanni" coarse (No.11416), extrafine calcite (No.58720), and rabbit glue pearls (No.63028). According to the manufacturer, the average pigment particle size was <120 μm, 120 μm - 1 mm, and ~20 μm, respectively. Note that "Bianco di San Giovanni" was historically prepared by sun-drying small "cakes" of slaked lime to achieve a partial carbonation of $Ca(OH)_2$ [4]. Consequently, this pigment contains a mixture of calcium hydroxide and calcium carbonate of varying proportions, depending on the preparation method. Additionally, analytical grade calcium hydroxide ($Ca(OH)_2$, Guinama S.L.U., Spain) and calcium carbonate ($CaCO_3$, Labkem, Spain) were included in this study as reference materials.

2.2. Sample preparation

Two sets of dosimeters were prepared. The first set of samples was prepared following traditional medieval recipes according to organoleptic parameters in order to obtain paints with adequate consistency [11,12]. Since binder demand depends on the pigments' chemical composition and particle size, these paints contained varying amounts of binder (see TG results below). Rabbit glue pearls (8 g) were soaked in 100 ml deionized water for 24 h under occasional stirring before heating to just below 50 °C in a water bath until a homogeneous mixture was obtained. To prepare a tempera paint of appropriate consistency, pigments were first wetted with deionized water and afterwards mixed with sufficient animal glue paste. Dosimeters were prepared by applying paints as well as pure rabbit glue paste on glass slides using a brush. The dosimeters' dimensions were 15x20 × 1 mm. This set of samples was long-term exposed under ambient conditions at two locations in the city of Granada (see below for details).

The second set of samples was prepared in a similar fashion. However, the pigment-binder ratio was maintained constant at 10:1 wt/wt. This ratio has been chosen because it is close to the average binder content of paint dosimeters prepared according to traditional recipes and used for outdoor-exposure. In practice, 5 g of pigment was wetted with 4 g of deionized water and afterwards mixed with 6.5 g of rabbit glue paste (solid content 0.5 g). For comparison, samples made of 5 g calcium hydroxide mixed with 10 g of deionized water (without the addition of rabbit glue) were prepared. This set of samples was exposed to accelerated photo-aging in the laboratory (see below). Note that no attempt was made to study paints based on calcite-water mixtures, because drying resulted in a powdery pigment layer without any cohesion. Paint dosimeters are named according to the following system: A-B–C-D; A = type of pigment, B = particle size, C = type of binder, and D = type of exposure/location and duration. See Table 1 for the complete nomenclature of samples.

2.3. Outdoor exposure test

Paint dosimeters were placed in a semi-open courtyard of the Alhambra monument ("Patio del Harem", Nasrid palaces) and on a balcony (first floor) of a residential building facing SW adjacent to a highly trafficked street in the historic city center of Granada. Whereas dosimeters were protected from direct sunlight and rain at the Alhambra, they were exposed to rain and sunlight (~5 h daily in winter and ~10 h daily in summer) at the location in the city center. After the 24-month outdoor exposure the overall sunlight exposure duration was estimated to be ~5800 h at an irradiance level of ~1090 W/m^2 [13].

During the outdoor exposure tests, the maximum *T* in summer and minimum *T* in winter were 40 °C and −3 °C, respectively, with diurnal variations of up to 20 °C. Diurnal relative humidity (RH) variations reached 50% with average RH ranging from ~40% in summer to ~75% in winter. The number of rainy days per month varied between 0 and 14 (Fig. 1) [14].

Granada is a non-industrialized city. However, particulate matter, NO_2, and O_3 concentrations frequently exceed threshold values [15] set by the EU directive 2008/50 EC [16]. Particulate matter is expected to deposit on exposed painted surfaces, causing soiling. According to Urosevic et al. [17] its main constituents at Granada are: soil dust (quartz, calcite, dolomite, phyllosilicates, and iron oxides/hydroxides), black carbon, secondary inorganic aerosols, and sea salt.

2.4. UV-aging test

Dosimeters were exposed in the laboratory to UV-C radiation emitted by a small tubular Pen-Ray Mercury Lamp (No. 90-0012-01, Utra-Violet Products Ltd, UK). The lamp emits a spectrum with the

Table 1
Nomenclature of samples.

Pigments	
Cal-EF	Extrafine calcite
BSG-ST	Bianco di San Giovanni (standard)
BSG-C	Bianco di San Giovanni (coarse)
$CaCO_3$	Analytical grade calcium carbonate
$Ca(OH)_2$	Analytical grade calcium hydroxide
Outdoor exposed dosimeters	**Location and test duration**
Cal-EF-RG-A[a]	A = Alhambra
BSG-ST-RG-A	Test duration: 6, 12, and 24 months
BSG-C-RG-A	
Cal-EF-RG-CC	CC = city center
BSG-ST-RG-CC	Test duration: 6, 12, 24, and 30 months
BSG-C-RG-CC	
UV-aged dosimeters	
Cal-EF-RG-UV	Total test duration: 1000 h
BSG-ST-RG-UV	
BSG-C-RG-UV	
$CaCO_3$-RG-UV	
$Ca(OH)_2$-RG-UV	
$Ca(OH)_2$-H_2O-UV	

[a] All pigments are mixed with rabbit glue (RG) except $Ca(OH)_2$–H_2O which is mixed with water.

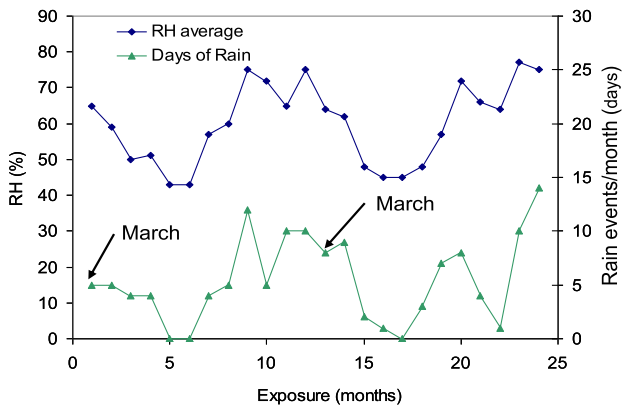

Fig. 1. Average RH (city center) and rain events per month during the 24-month outdoor exposure [14].

primary energy at 254 nm (2800 μW/m^2 UV-C irradiance at ~2.5 cm). During testing, paint dosimeters were placed in a chamber at 17 ± 4 °C and 50 ± 10% RH. Day-light was excluded using aluminum foil. The overall UV-exposure duration was 1000 h. Note that the UV-lamp was not operated continuously to prevent overheating and the UV-exposure was done over a 3-month period. For comparison a second set of samples was simultaneously placed in the chamber and protected from the UV-radiation by a cardboard, allowing for free air-circulation.

2.5. Analytical techniques

2.5.1. pH measurements

The pH of freshly prepared rabbit glue and paints was measured using a 905 Titrando coupled with a pH-meter (Electrode Plus, Metrohm AG, Switzerland).

2.5.2. Granulometry

A laser particle size analyzer (Mastersizer 2000LF, Malvern Instruments) was used to measure the particle size of calcium-based pigments dispersed in ethanol.

2.5.3. X-ray diffraction (XRD)

X-ray diffraction (X'Pert PRO PANalytical B.V.) was used to determine the mineralogical composition and evolution of calcium-based pigments and paint dosimeters. Analyses were performed using Cu-Kα radiation (λ = 1.5405 Å), Ni filter, 45 kV voltage, and 40 mA intensity, 3°-60° 2θ exploration range, and 0.05° 2θ s^1 goniometer speed. Xpowder software [18] was used to identify mineral phases and perform semi-quantitative analyses.

2.5.4. Thermogravimetric (TG) analysis

The rabbit glue content of paint dosimeters prepared according to traditional medieval recipes, before and after outdoor exposure, was determined using a Shimadzu TGA-50H (Shimadzu Corporation). Analysis conditions: flowing air (100 ml/min) and a constant heating rate of 10 °C min^{-1} (25-950 °C). In order to calculate the dosimeters' binder content, the weight loss of the corresponding calcium-based pigment and pure rabbit glue in the same T range were considered. Note that the full T range was considered in the case of blank dosimeters and dosimeters exposed at the Alhambra because these samples did not undergo significant mineralogical changes due to carbonation. In the case of dosimeters prepared with BSG and exposed in the city center, in contrast, only the T range between 330 and 600 °C was considered because they underwent significant carbonation according to XRD results (see below). At $T < 330$ °C dehydration of amorphous calcium carbonate (i.e., ACC is a precursor of calcite and forms upon carbonation of $Ca(OH)_2$) can contribute to weight loss, whereas at $T > 600$ °C decomposition of calcite can be expected [19]. Neglecting both reactions would lead to an overestimation of the binder content.

2.5.5. Stereomicroscopy

Textural, structural and chromatic features of blank and aged paint dosimeters were determined using a stereomicroscope (SMZ 1000, Nikon).

2.5.6. Spectrophotometry

A portable spectrophotometer (Minolta CM-700d) was used to determine color changes of dosimeters before and after UV-aging and outdoor exposure. Equipment settings were: illuminant D65, 10° observer, Ø 6 mm measurement area. Data were expressed in CIE L*a*b* and CIE L*C*h* color spaces (i.e., L* is luminosity or lightness (black = 0 and white = 100)); a* from +a* (red) to −a* (green), and b* from +b* (yellow) to −b* (blue), C* is chroma or saturation, and h* is hue. Color changes for L*, a*, b*, C*, and ΔE were calculated. The latter was calculated using the following formula: $\Delta E=(\Delta L^{*2}+\Delta a^{*2}+\Delta b^{*2})^{1/2}$. Average values are based on a minimum of 5 measurements per sample. Note that a color difference of ΔE ≥3 is perceptible to the human eye [20].

2.5.7. Attenuated total reflectance – Fourier transform infrared spectroscopy (ATR-FTIR)

Mineralogical changes of calcium-based pigments and conformational changes of the rabbit glue were studied using ATR-FTIR spectroscopy (Jasco 6200, JASCO Analytical Instruments, Japan). Small powder samples of blank and aged paints and binder were analyzed at a 2 cm^{-1} resolution over 75 scans from 400 to 4000 cm^{-1}.

2.5.8. Field emission scanning electron microscopy (FESEM)

Morphological features of pigments and dosimeters were studied using a FESEM (Auriga, Carl Zeiss, Germany) working at 10^{-4} Pa vacuum and 3 kV in secondary electron imaging mode. Samples were carbon coated.

3. Results and discussion

3.1. pH measurements

The rabbit glue had a slightly acidic pH which lowered the pH of the binary paint systems with respect to the original equilibrium pH of these pigments in saturated aqueous solutions (Table 2). Note that the pH of saturated $Ca(OH)_2$ and $CaCO_3$ solutions are ~12.5 and ~9, respectively. The high pH of paints containing $Ca(OH)_2$ can have

Table 2
pH of freshly prepared paints with rabbit glue or water.

Paint sample	pH
Cal-EF-RG[a]	7.7
BSG-ST-RG	11.1
BSG-C-RG	11.5
$CaCO_3$-RG	6.6
$Ca(OH)_2$-RG	11.6
$Ca(OH)_2$-H_2O	12.4
Rabbit glue	5.8

[a] See Table 1 for sample nomenclature.

important effects on the organic binder. At high pH carboxyl and amine groups of the protein binder are deprotonated. However, only the former will be involved in the formation of complexes with Ca^{2+} [21]. Considering the higher solubility of $Ca(OH)_2$ (1.73 g/L (20 °C)) as compared to calcite (0.013 g/L (25 °C)), the formation of organo-metal complexes (i.e., one Ca^{2+} ion coordinated to two carboxyl groups) in an aqueous solution will be much more likely in BSG/portlandite-based paints than in those based on calcite [7]. Denninger [5] recognized that $Ca(OH)_2$ reacted with protein to form protein-lime compounds which were especially stable in the case of lime-casein mixtures where calcium caseinate compounds formed.

However, high pH can also cause unfolding and denaturation of the proteinaceous binder [22] (Das 2005). This process affects the secondary structure of proteins, resulting in a partial or total loss of regular repeating patterns such as beta-sheets or alpha-helices by disruption of noncovalent bonds [23] (see FTIR results below). High pH is also likely to cause modification of the protein backbone structure by breaking covalent peptide bonds between carboxyl and amino groups upon hydrolysis. Alkaline hydrolysis of proteins, thus, results in their breakdown into individual amino acids [24].

Moreover, when used in conservation interventions, the high pH of tempera paints prepared with BSG pigments has to be considered if mixed with alkaline-sensitive pigments such as Prussian blue, verdigris, chrome yellow, crimson lake, and zinc white because undesired color changes might occur [1].

3.2. Particle size analysis of calcium-based pigments

Analytical results revealed a relatively wide particle size range for all pigments with a variable contribution of nano-sized particles (Fig. 2). The different pigment particle sizes had a strong influence on the surface finish of the tempera paints, larger particle sizes resulting in a much rougher, irregular surface (Fig. 3).

3.3. XRD analysis of pigments and paint dosimeters

3.3.1. Pigments

Semiquantitative X-ray analysis of pigments showed that both BSG pigments contained large amounts of portlandite (85 wt%) and only ~15 wt% calcite had formed upon reaction with ambient CO_2 during the preparation of this commercial pigment. The portlandite content of these pigments is significantly higher than that reported by Denninger [5]. This author prepared "Bianco di San Giovanni" according to a recipe by Cennini and obtained a pigment with ~70% calcite content. These results indicate that the preparation method and the environmental conditions (i.e., *T* and RH) during preparation will have an important influence on the pigment's calcite content.

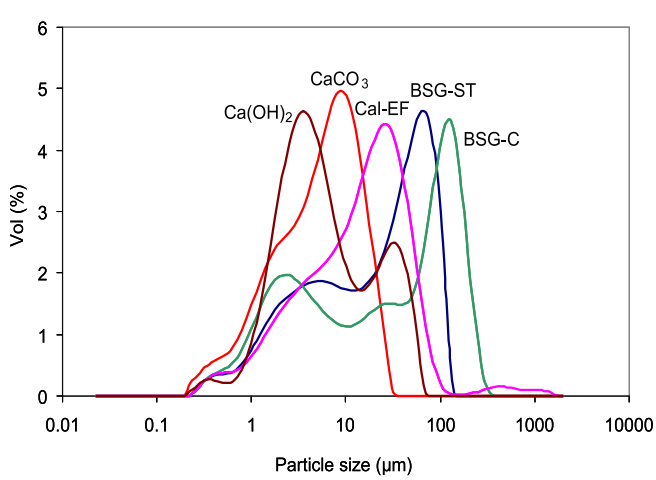

Fig. 2. Particle size distribution (μm) of calcium-based pigments. (see Table 1 for sample nomenclature).

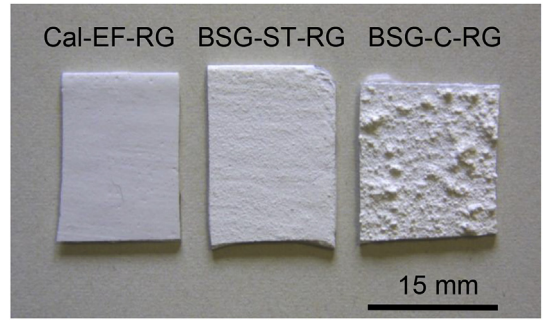

Fig. 3. Macroscopic surface texture of blank paint dosimeters (see Table 1 for sample nomenclature).

The commercial extrafine calcite (Cal-EF) pigment contained ~10 wt% dolomite and a trace amount of quartz, whereas analytical grade calcite revealed no impurities detectable with this technique. The analytical grade calcium hydroxide contained <5 wt% calcium carbonate.

3.3.2. UV-aging of paint dosimeters

The mineralogical composition of calcium-based tempera paints did not change qualitatively during accelerated aging. XRD results, however, revealed that the organic binder had an important effect on the carbonation rate of BSG/$Ca(OH)_2$-based paints (Fig. 4). Note that in Fig. 4 only $Ca(OH)_2$-based paints are included as BSG-based paints showed a very similar behavior to $Ca(OH)_2$-based paints upon carbonation and no mineralogical changes due to carbonation are expected in Cal-EF and $CaCO_3$-based paints. Carbonation was much slower in the presence of rabbit glue, which, apparently, acted as a carbonation inhibitor, impeding the diffusion of ambient CO_2 by forming a superficial film around portlandite particles. Its possible role as a crystallization inhibitor (i.e., delaying nucleation and growth) of calcium carbonate phases cannot be ruled out either. Consequently, the degree of carbonation reached after 3 months in BSG/$Ca(OH)_2$-based paints mixed with rabbit glue was much lower than in $Ca(OH)_2$-paint dosimeter prepared with H_2O, which showed an initial fast carbonation, slowing down drastically after ~75 wt% of portlandite had carbonated. The reason for the slowing of carbonation is threefold: (1) Carbonation is a decelerator process because it proceeds from the outside inward, thus, the distance to the carbonation front increases as the carbonation proceeds [19]. (2) Pore space is partially filled upon $CaCO_3$ precipitation which significantly hinders CO_2 diffusion [25]. (3) The carbonation requires water. It proceeds according to the following overall reactions [26]:

$$Ca(OH)_2\,(s) + CO_2\,(g) + H_2O\,(aq) \rightarrow CaCO_3\,(s) + 2H_2O\,(aq) + \text{heat} \uparrow (74\ \text{kJ/mol}) \quad (1)$$

Beruto et al. [27] were able to demonstrate that $Ca(OH)_2$ was significantly more hygroscopic than $CaCO_3$, adsorbing nearly twice as much water at 50% RH. The authors found that water started to leave the reaction zone when about 85 wt% of $Ca(OH)_2$ had carbonated, thus slowing down the reaction. This effect explains the drastic reduction in the carbonation rate we observed when 75 wt% of $Ca(OH)_2$ had carbonated (Fig. 4).

UV-exposure accelerated carbonation in paints containing

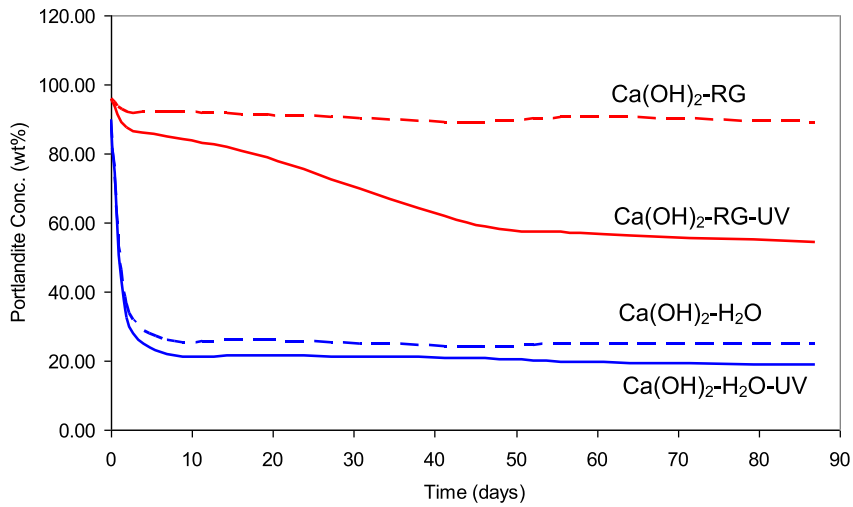

Fig. 4. Portlandite (wt%) concentration versus time of UV-aged and non UV-aged paint dosimeter with and without organic binder. RG = rabbit glue.

organic binder, especially during the initial stage. Results suggest that acceleration was caused by a photo-induced partial degradation of the organic binder, facilitating the diffusion of CO_2 towards the carbonation front. The 5% higher degree of carbonation reached in UV-exposed samples prepared by mixing $Ca(OH)_2$ with water as compared to the sample protected from UV-radiation is not considered statistically significant. Note that XRD only allows for a semi-quantitative analysis of mineral phases with an accuracy of ±5%.

3.3.3. Outdoor-exposure of paint dosimeters

XRD results of samples exposed for 24 months showed very little changes in the case of dosimeters prepared with extrafine calcite. Only the quartz content seemed to have increased slightly as a result of particulate matter deposition [17]. A similar effect was observed in all outdoor exposed dosimeters. Additionally, dolomite was detected in outdoor exposed dosimeters prepared with BSG pigments which did not contain dolomite before exposure. The dolomite concentration increased over time and can as well be associated with particulate matter deposition [17].

Dosimeters prepared with BSG pigments suffered additional mineralogical changes, which depended on environmental conditions during outdoor exposure (Fig. 5). The sheltered samples exposed at the Alhambra carbonated slower as compared with the unsheltered ones placed in the city center which were completely carbonated after 6 months. Carbonation is a dissolution-precipitation reaction and water is, thus, required (see reaction (I)). In both outdoor locations water can be adsorbed from the atmosphere at sufficiently high RH. However, at low RH carbonation will slow down or even cease at RH <30% [28]. In the case of samples exposed in the city center, additional water is supplied by the direct impact of rain, thus, facilitating carbonation. Furthermore, binder loss was more severe in dosimeters exposed in this latter location (see TG results below) as a result of the direct impact of rain and sunlight. In the case of the sheltered samples at the Alhambra, in contrast, almost all binder was still retained after 6 months (see TG and SEM results below) and it is, thus, not surprising that even after 24 months BSG-ST-RG-A and BSG-C-RG-A still contained 20 and 30 wt% of calcium hydroxide, respectively. Carbonation also depends on particle size (i.e., it will take longer until the core of larger aggregates is fully carbonated [29]), and it is, thus, not unexpected that a higher degree of carbonation was achieved in dosimeters prepared with the finer-grained BSG-ST than in the ones prepared with BSG-C.

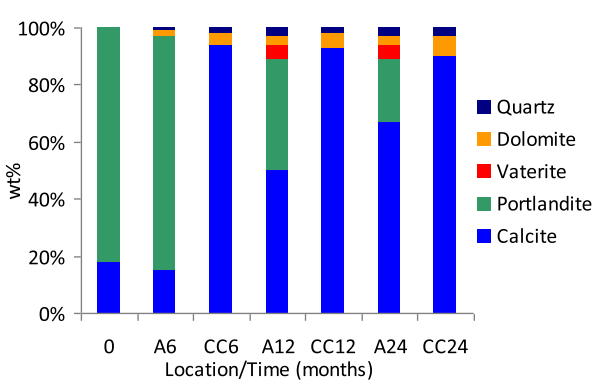

Fig. 5. Evolution of the mineralogical composition over time of BSG-ST-RG paint dosimeter exposed at the Alhambra (A) and the city center (CC) of Granada for different periods of time (0, 6, 12, and 24 months).

The different environmental conditions did not only affect the carbonation rate and yield. XRD results revealed that the presence of a significant amount of rabbit glue in BSG-ST-RG-A and BSG-C-RG-A exposed at the Alhambra facilitated the stabilization of vaterite, which was detected after 6 and 12 months (Fig. 6), respectively. Note that vaterite, a polymorph of calcium carbonate and precursor of calcite, is unstable under most conditions because of its higher solubility and lower density as compared to calcite [30]. It is, however, stabilized in the presence of organic polymeric substances, including those containing amino acids [31,32]. According to XRD data, metastable vaterite transformed into calcite at a very slow rate (i.e., vaterite was still present in samples exposed for 24 months at the Alhambra). This is consistent with previous studies, showing a kinetic stabilization of vaterite in the present of organic additives, which prevented or delayed its transformation into calcite [33]. Regarding mechanical resistance, metastable phases such as vaterite are less desirable as compared to the interlocked structure of calcite (see FESEM results below). Furthermore, mineralogical changes are accompanied by volumetric changes. Table 3 shows that the transformation from portlandite to vaterite will result in a volume increase of 19%. This increase is almost twice as high as the volume increase corresponding to the transformation of portlandite into calcite. It is especially important, considering the relatively large amount of

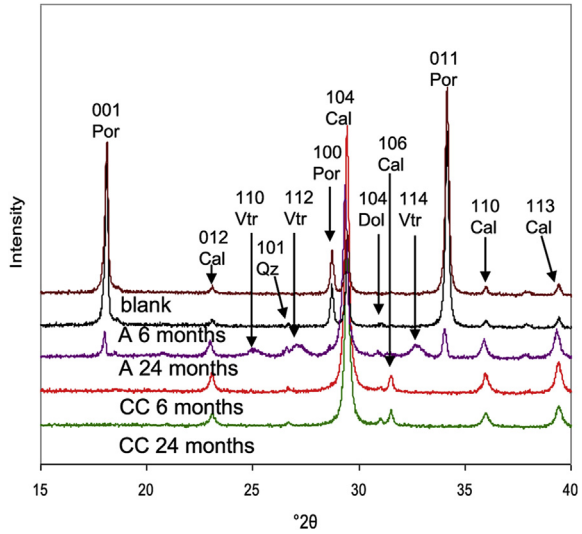

Fig. 6. Diffractograms of a blank BSG-ST-RG dosimeter and the same dosimeters exposed at the Alhambra and the city center for 6 and 24 months. Por = portlandite, Qz = quartz, Vtr = vaterite, Cal = calcite.

Table 3
Molar volume (cm^3 mol^{-1}) of minerals and calculated volume change (%) upon phase transition.

Mineral	Molar volume (cm^3 mol^{-1})	Volume change (%)
Por	33.2	19 (Por→Vtr)
Vtr	39.4	−6 (Vtr→Cal)
Cal	36.9	11 (Por→Cal)

Por = portlandite, Vtr = vaterite, Cal = calcite.

portlandite present in the commercial BSG pigments studied here.

3.4. FESEM analysis of pigments and paint dosimeters after accelerated UV-aging and outdoor exposure

3.4.1. UV-aging test

According to FESEM observations the presence of the organic binder influenced significantly the morphological evolution of $Ca(OH)_2$ (Fig. 7). As indicated by XRD analysis, the organic binder reduced the carbonation rate and aggregates of nano-sized particles were detected which did not differ significantly from those of the original $Ca(OH)_2$ sample (Fig. 7a and b). Additionally, some hexagonal portlandite crystals were present (Fig. 7b, arrow). Both, the irregular nano-sized and the hexagonal plate-like morphologies are typical of portlandite crystals in slaked lime [34]. In samples prepared with water, in contrast, faster carbonation occurred according to XRD results and the formation of calcite crystal bundles with the typical scalenohedral morphology (Fig. 7c) was observed.

3.4.2. Outdoor exposure test

3.4.2.1. Cal-EF-based paints. FESEM images of dosimeters prepared with extrafine calcite (Cal-EF) (Fig. 8) revealed the presence of large amounts of rabbit glue binder, partially filling pores and connecting crystal grains after 6 months of outdoor exposure at the Alhambra (Fig. 8b). More prolonged outdoor exposure up to 24 months did not induce chemical weathering of calcite. Crystal faces remained intact and did not show any signs of dissolution if compared to the unweathered pigment (Fig. 8a and c). However, fracturing of the rhombohedral calcite crystals along {104} cleavage planes was observed which likely was induced by severe diurnal *T* changes (Fig. 8c). It is known that calcite is prone to physical weathering due to thermal cycling, a deleterious phenomenon associated with the anisotropic thermal expansion of calcite crystals [35]. Note that paint samples were not ground prior to FESEM analysis. Thus, fracturing was no artifact of sample preparation. It is not surprising that the calcite-based pigment did not undergo any compositional or important morphological changes upon mixing with rabbit glue and during the long-term exposure of the paint dosimeters at the Alhambra. The pigment only acted as filler in the tempera paint. Considering the low solubility of calcite, binding between deprotonated carboxyl groups of amino acids and Ca^{2+} is very limited and significant adsorption or incorporation of organics into the calcite crystals cannot be expected either. Consequently, the binder can be easily leached out upon rain- and sunlight exposure (see TG results below).

3.4.2.2. BSG–based paints. FESEM images of both, standard and coarse BSG pigments (Fig. 9a and d) revealed that they were constituted of nano-sized primary particles which formed larger aggregates of portlandite and calcite crystals. After 6-month exposure at the Alhambra (Fig. 9b), particle morphology did not change significantly, confirming XRD results which showed no important increase in the calcite content due to carbonation of portlandite. Large amounts of rabbit glue, binding pigment grains, were detected in the same sample. These findings suggest that in the presence of the organic binder and under the prevailing environmental conditions of the sheltered location at the Alhambra, important portlandite dissolution and calcite precipitation did not occur during the first 6 months of exposure. After prolonged exposure for up to 24 months at the Alhambra, solid and hollow sphere-shaped morphologies, the latter partially collapsed, were detected (Fig. 9c). These morphologies are typical of both, ACC and vaterite [36,37]. Vaterite was actually identified with XRD in these

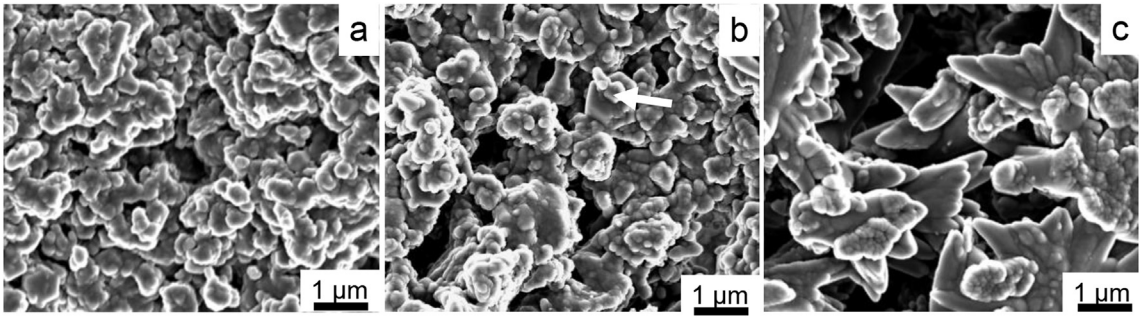

Fig. 7. FESEM images of (a) pure $Ca(OH)_2$ and dosimeters (b) prepared with $Ca(OH)_2$ and rabbit glue (arrow indicates hexagonal portlandite crystal) or (c) with $Ca(OH)_2$ and water after 1000 h UV-aging/3 months at 50 ± 10% RH.

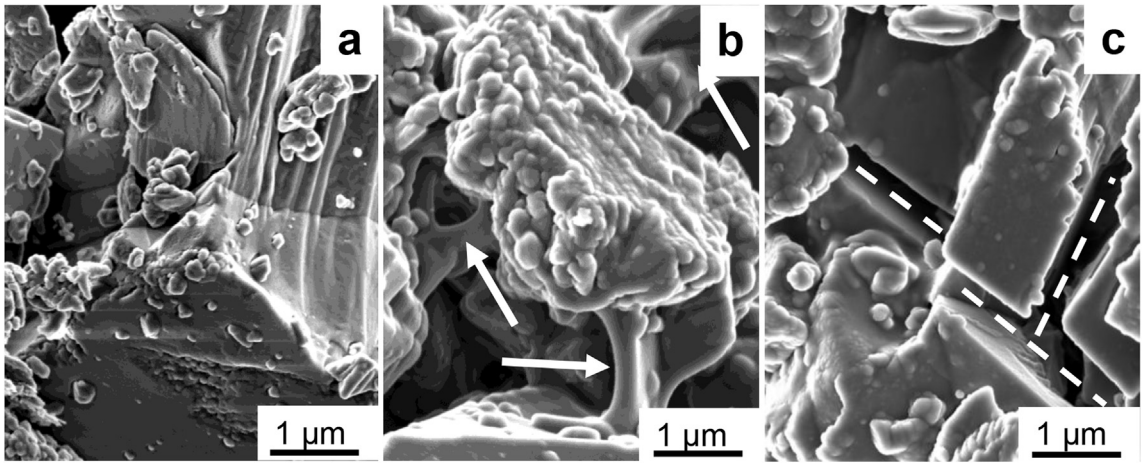

Fig. 8. FESEM image of (a) original Cal-EF pigment; (b) dosimeter prepared with Cal-EF after 6 months exposure at the Alhambra (arrows indicate rabbit glue binder); (c) same sample after 24-month exposure at the Alhambra (dashed lines show fractures along {104} planes in rhombohedral calcite crystals).

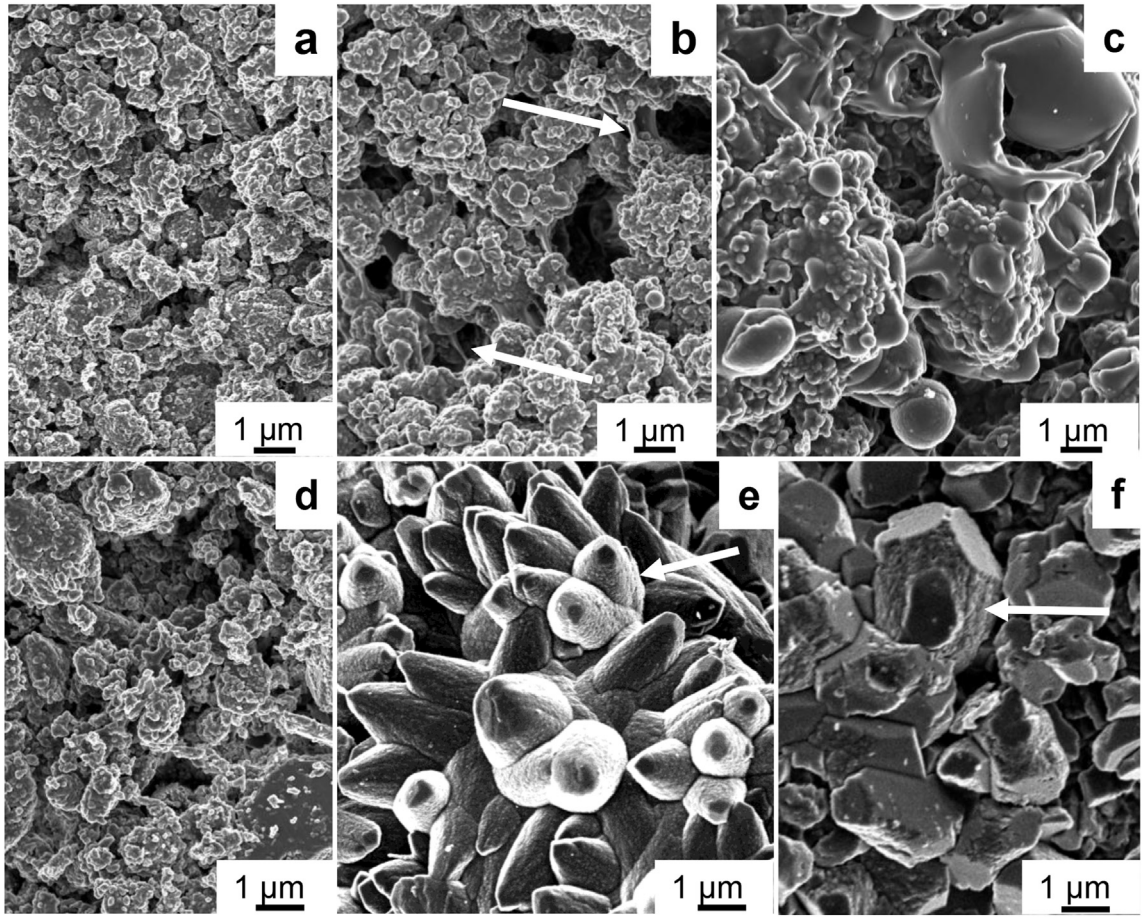

Fig. 9. FESEM images of (a) original BSG-ST pigment; (b) dosimeter prepared with BSG-ST after 6 months exposure at the Alhambra (arrows indicate rabbit glue binder); (c) the same sample after 24-month exposure at the Alhambra showing spherical morphologies typical for amorphous calcium carbonate and vaterite; (d) original BSG-C pigment; and dosimeter prepared with BSG-C after 6-month (e) and 12-month (f) exposure in the city center (arrows indicate rounded edges of organic-calcite composite material).

samples. As mentioned above, ACC and vaterite are precursors of calcite and known to be stabilized in the presence of organics. From a mechanical point of view the formation of these spherical phases is less desirable as compared to interlocked scalenohedral calcite crystals [38], because they are metastable and less dense and confer lower cementing capacity at an early stage of carbonation. After 24 months of exposure at the Alhambra, aggregates of nano-sized particles similar to those observed in slaked lime were still detected in BSG-ST-RG and BSG-C-RG, which is in agreement with XRD results revealing the presence of 20 and 30 wt% of portlandite, respectively.

BSG samples exposed in the city center of Granada showed

drastic morphological changes as a result of a complete carbonation of portlandite (Fig. 9e and f). Scalenohedral calcite crystals, commonly known as dogtooth spar, were observed after 6 months of exposure. Scalenohedral crystals typically form during carbonation of $Ca(OH)_2$ under excess Ca^{2+} ions (i.e., $Ca^{2+}/CO_3^{2-} \gg 1$) and high pH [38]. However, the presence of the organic binder modified the typical straight edges of rhombohedral or scalenohedral calcite faces to rounded less well defined edges. It has been reported that different organics can be adsorbed at specific, non-structurally equivalent steps of calcite crystals, leading to step pinning which results in the rounding of the grow steps [39]. This is manifested macroscopically by the change in crystal morphology (i.e., edge rounding and development of forbidden faces [40] observed here). Cho et al. [41] showed that these organics are even incorporated within the calcite structure. The observed morphologies are consistent with the formation of new organic-inorganic composite materials, mimicking biominerals, which generally have improved physical-mechanical properties, being both harder and more fracture resistant compared with their inorganic counterparts [42]. Recent experimental results also show that $CaCO_3$ biominerals are more resistant to chemical weathering (i.e., dissolution) than pure calcite [43]. Overall, the formation of such hybrid organic-inorganic $CaCO_3$ structures helps explain why BSG based paints show a high durability even under the harsh exposure conditions faced in the city center of Granada.

3.5. TG analysis

TG results (Table 4) revealed a higher binder content in unaltered dosimeters prepared with BSG pigments as compared to extra-fine calcite. It is commonly accepted that finer grained pigments have higher binder demand than coarse grained ones and, according to particle size analyses, the BSG pigments had a much larger average particle size than the extra-fine calcite. However, FESEM images (see above) revealed that the large grains in BSG pigments consisted of aggregates of nano-sized $Ca(OH)_2/CaCO_3$ primary particles, which partially disaggregated when mixed with rabbit glue, leading to the increase in binder demand observed here.

Analytical results of outdoor exposed paint dosimeters showed that binder loss was negligible in samples exposed at the Alhambra (Table 4). The apparently slightly higher binder content in the coarse BSG-C-RG-A sample exposed for 6 months at the Alhambra as compared to the blank dosimeter is possibly caused by the presence of ACC. Note that ACC which systematically forms during the carbonation of portlandite [19] cannot be detected with XRD. It dehydrates between 100 and 350 °C [19] and, thus, contributes to weight loss in the temperature range where decomposition of organic binder occurs. In samples exposed in the city center which suffered the direct impact of rain and sunlight, important binder loss between 50 and 65% was detected. Binder loss was 15 wt% higher in the dosimeter prepared with extrafine calcite than in the ones prepared with BSG pigments. As mentioned earlier, extrafine calcite only acts as filler and the water-soluble rabbit glue binder can be easily leached out. Lower binder loss in BSG-based paints can be explained by the formation of composite materials similar to biominerals (see FESEM results above). Biominerals commonly contain only a few wt percent of the organic component [42], which is sufficient to drastically increase their hardness and strength, as well as their resistance to chemical weathering [43]. Thus, it is concluded that only a small part of the organic binder is actually incorporated into the calcite crystal structure, whereas the rest of the remaining rabbit glue is protected from leaching by the newly formed interlocked structure of calcite crystals. These results suggest that the weathering resistance of fully carbonated tempera paints prepared with BSG pigments is much higher than that of paints prepared with Cal-EF pigments. Photographic evidence (Fig. 10) and quantitative image analysis (Table 4) of paint dosimeters exposed for 30 months at the city center confirms this hypothesis. Only trace amounts of Cal-EF-RG paint remained on the glass slide, whereas paint films prepared with BSG-based paints had suffered only minor material loss.

Table 4
Rabbit glue binder content in tempera paint dosimeters.

	Binder content (wt%)	Binder loss (%)	Paint loss (%)[a]
Blank dosimeters			
Cal-EF-RG[b]	8.4		
BSG-ST-RG	16.0		
BSG-C-RG	14.3		
Outdoor exposure at the Alhambra		6 months	
Cal-EF-RG-A6	8.4	0	0
BSG-ST-RG-A6	14.5	−9	0
BSG-C-RG-A6	16.2	+13.3	0
Outdoor exposure in the city center		6 months	
Cal-EF-RG-CC6	2.9	−66	>99
BSG-ST-RG-CC6	8.3	−48	8
BSG-C-RG-CC6	7.3	−50	<1

[a] After outdoor exposure for 30 months, calculated using image analysis of photographic images (Fig. 10).
[b] See Table 1 for sample nomenclature.

3.6. FTIR-ATR spectroscopy of pure rabbit glue and calcium-based paints

3.6.1. Rabbit glue binder

Spectroscopic results revealed a blue shift of the amide I band from 1627 to 1637 cm^{-1} of pure rabbit glue after UV-aging (Fig. 11). This shift does not indicate significant conformational changes and the band was assigned to a β-sheet structure [44]. The amide II band suffered a shift from 1539 to 1525 cm^{-1} in pure rabbit glue. A similar shift has been reported upon thermal denaturation of parchment [45] and is possibly induced by cross-linking [46]. The formation of covalently cross-linked polymers during photo-oxidation is the likely cause for yellowing of organic polymers [47] which was actually observed in the case of pure rabbit glue (see color measurements below).

Upon mixing of the rabbit glue with calcium-based pigments and prior to aging, the amide I band of the proteinaceous binder shifted from 1627 to 1647 cm^{-1} regardless of the pigments' mineral composition, particle size and pH. This shift indicates an important change in the conformational structure, now being assigned to random coil [44]. According to Von Endt et al. [7], the presence of a

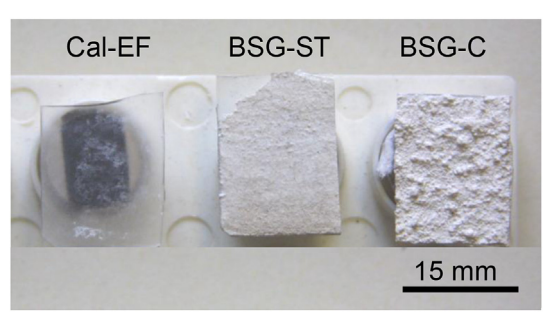

Fig. 10. Photographic image of dosimeters exposed in the city center for 30 months showing an almost complete loss in the case of Cal-EF-based paint.

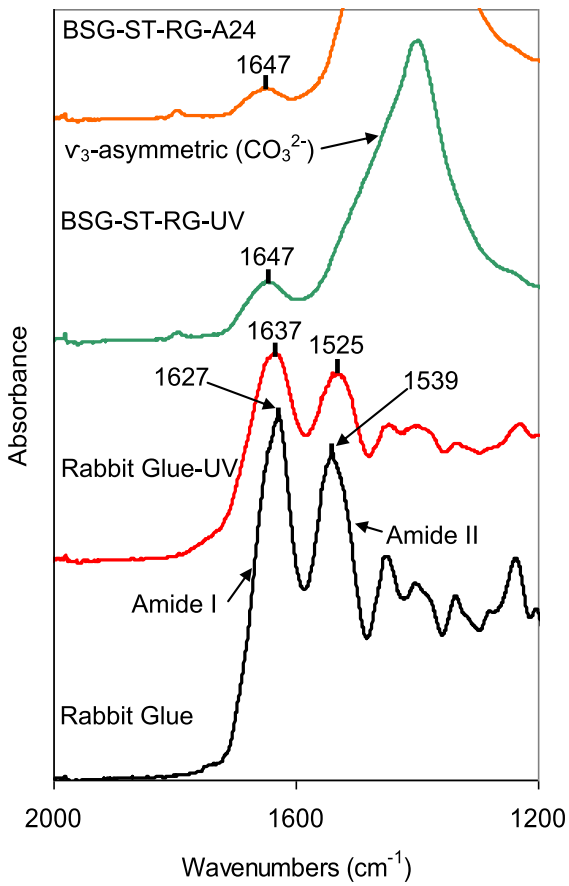

Fig. 11. FTIR position of the Amide I and II band in rabbit glue before and after UV-aging and in dosimeters prepared with BSG-ST-RG after UV-aging and outdoor exposure at the Alhambra for 24 months. RG = rabbit glue.

filler (e.g. calcium carbonate) in animal glue will impede the realignment of the collagen chains into their original 3-coil structure and chains remain in a "spread-out configuration" (i.e., random coil).

UV-aging and 24-month outdoor exposure did not cause any further shift in the amide I band and a possible shift of the amide II band cannot be determined in calcium-based tempera paints because the band is masked by the intense v_3-asymmetric (CO_3^{2-}) stretching (Fig. 11). Thus, it was not possible to correlate the observed photo-induced color change of Ca-based paints during UV-aging and outdoor exposure (see below) with conformational changes in the organic binder.

3.6.2. Pigments

FTIR data confirmed XRD results regarding the mineralogical composition of calcium-based tempera paints (Fig. 12). Note that the spectrum of altered rabbit glue is included in Fig. 12 in order to indicate the amide I and II band positions. The spectrum of pure $Ca(OH)_2$ mixed with water showed a drastic intensity decrease of the v(OH) band (O–H stretching) and an intensity increase of the v_4-symmetric (CO_3^{2-}) band as compared to the same sample mixed with rabbit glue, indicating an important degree of carbonation in the former. In the spectrum of $Ca(OH)_2$ mixed with rabbit glue, in contrast, the v_4-symmetric (CO_3^{2-}) band was barely visible. The strong v(OH) band points to the presence of large amounts of uncarbonated portlandite and, thus, to a low degree of carbonation (Fig. 12). In the $Ca(OH)_2$-RG sample, the shoulder of the v_3-asymmetric (CO_3^{2-}) band and its broadness suggest the presence of ACC, a precursor for crystalline calcium carbonate phases [48]. This finding confirms the retardation action of rabbit glue on the carbonation of portlandite and the stabilization of metastable phases such as ACC. Under normal conditions the highly soluble and unstable ACC readily transforms to vaterite or calcite. However, the stabilization of ACC has been observed in a wide range of biominerals in the presence of organics [36,49].

3.7. Color parameters of pure rabbit glue, calcium-based pigments and paints

3.7.1. UV-aging test

UV-aging for 1000 h caused only minor color changes in paint dosimeters, the ΔE values not exceeding 3 units. However, the pure rabbit glue sample underwent drastic yellowing (i.e., b* increased by ~14 units) as well as a reduction in lightness and an increase in saturation (Table 5), which is likely caused by protein denaturation detected with FTIR analysis [47]. Remarkably, only a minor yellowing of the calcium-based tempera paint was observed in a few samples (i.e., yellowing was slightly more pronounced in Cal-EF-RG and BSG-ST-RG) and did not reveal any relationship with the pigments' mineralogical composition or particle size.

Experimental results obtained during UV-aging clarified the possible effect of mineralogical and morphological changes on the paints' optical properties. It is generally accepted that the light-scattering of pigments depends on mineralogy (i.e., refractive index, particle size, size distribution, and shape [50]). All these parameters are modified during the carbonation process undergone by portlandite. In the case of $Ca(OH)_2$–H_2O the dosimeter did not contain any organic binder which could have degraded and contributed to the change of the samples' optical properties. The fact that no change in the color parameters was detected in the $Ca(OH)_2$–H_2O sample where, according to XRD, 80% of the portlandite carbonated after the 1000 h UV-aging, suggests that morphological changes did not account for any important changes in the optical properties.

3.7.2. Outdoor-exposure test

Color measurements prior to outdoor exposure showed that the pigments lightness was reduced when mixed with the organic binder. Additionally, an important increase in b* and saturation was observed, the former being caused by the slightly yellow color of the pure rabbit glue (Table 6). Experimental data revealed that the optical properties of outdoor-exposed calcium-based tempera paints were altered by various factors, namely binder alteration, binder loss and surface soiling. Furthermore, yellowing due to binder degradation was directly proportional to the binder content.

In Cal-EF-based tempera paints only minor yellowing due to binder alteration, indicated by a small increase in b*, was observed in samples exposed at the Alhambra where binder loss was very limited. These samples also suffered a reduction in lightness which can be related to soiling. Soiling was less severe in Cal-EF-based paints than in paints prepared with BSG-pigments due to the smoother surface in the case of the former. The effect of yellowing and soiling increased over time. However, color change never exceeded 3 units. In the city center where significant binder loss occurred, samples were actually slightly less yellowish than the corresponding blanks (i.e., Δb had negative values). The paint's lightness was not affected, possibly because deposited particulate matter did not adhere well to the smooth surface and was washed off by the direct action of rain.

BSG-based paints suffered a color change of ~4–7 units after 24 months of exposure, which was clearly perceptible to the human eye. The cause of the color change varied depending on the exposure conditions. In the case of dosimeters exposed at the Alhambra,

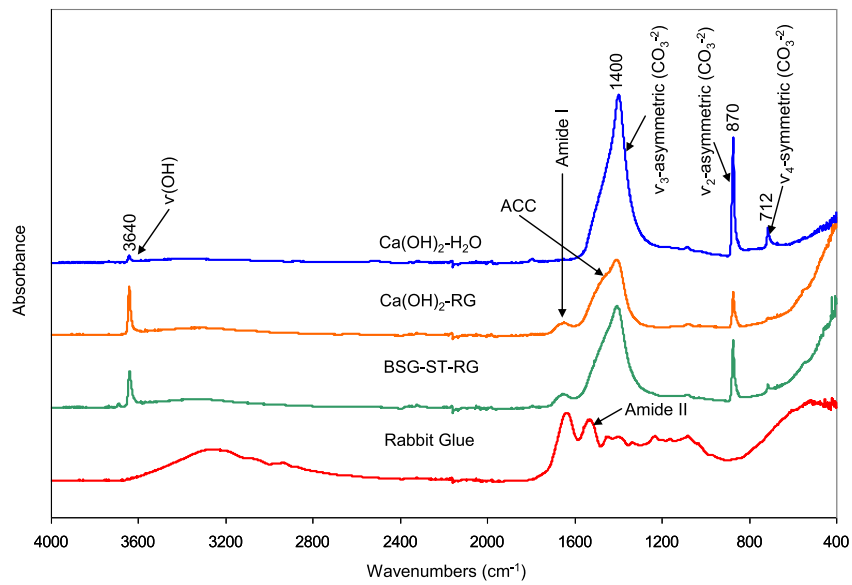

Fig. 12. FTIR spectra of rabbit glue and paint dosimeters after UV-aging for 300 h (equivalent to 1 month of carbonation). ACC = amorphous calcium carbonate, RG = rabbit glue.

Table 5
Lightness (L*), a* and b* parameters, h* (hue angle), and chroma (C*, relative saturation) for blank paint dosimeters, and dosimeters exposed to UV-aging for 1000 h.

	L*	a*	b*	h*	C*	ΔL	Δa	Δb	ΔC	ΔE
Rabbit Glue	78.75	−0.09	11.86	90.45	11.86					
	±0.28	±0.05	±0.27	±0.22	±0.27					
Rabbit Glue-UV	72.42	1.21	25.70	87.30	25.73	−6.33	1.31	13.84	13.87	15.28
	±0.21	±0.24	±0.23	±0.52	±0.23	±0.21	±0.24	±0.23	±0.23	±0.21
Cal-EF -RG	92.02	−0.33	3.11	96.02	3.13					
	±0.07	±0.02	±0.05	±0.26	±0.05					
Cal-EF-RG-UV	93.00	−1.42	5.78	103.75	5.96	0.98	−1.09	2.67	2.83	3.10
	±0.52	±0.26	±0.25	±2.01	±0.29	±0.52	±0.26	±0.25	±0.29	±0.16
BSG-ST-RG	95.62	−0.47	1.20	112.10	1.29					
	±0.46	±0.03	±0.28	±3.88	±0.27					
BSG-ST-RG-UV	97.47	−0.28	2.26	96.95	2.28	1.85	0.20	1.06	0.99	2.15
	±0.11	±0.02	±0.11	±0.31	±0.12	±0.11	±0.02	±0.11	±0.12	±0.07
BSG-C-RG	97.75	−0.16	2.55	93.70	2.56					
	±0.08	±0.02	±0.05	±0.40	±0.05					
BSG-C -RG-UV	97.35	−0.32	2.92	96.19	2.94	−0.40	−0.15	0.37	0.38	0.57
	±0.12	±0.03	±0.15	±0.49	±0.15	±0.12	±0.03	±0.15	±0.15	±0.18
$CaCO_3$-RG	94.22	−0.10	3.69	91.51	3.69					
	±0.27	±0.04	±0.25	±0.62	±0.25					
$CaCO_3$-RG-UV	94.97	−0.21	3.40	93.62	3.41	0.74	−0.11	−0.29	−0.28	0.99
	±0.37	±0.07	±0.49	±1.48	±0.49	±0.37	±0.07	±0.49	±0.49	±0.16
$Ca(OH)_2$-RG	96.76	0.26	3.44	85.74	3.45					
	±0.06	±0.01	±0.09	±0.19	±0.09					
$Ca(OH)_2$-RG-UV	96.43	0.05	3.90	89.31	3.90	−0.33	−0.21	0.46	0.46	0.61
	±0.05	±0.01	±0.05	±0.11	±0.05	±0.05	±0.01	±0.05	±0.05	±0.05
$Ca(OH)_2$-H_2O	97.02	0.21	2.40	84.89	2.41					
	±0.04	±0.02	±0.01	±0.35	±0.01					
$Ca(OH)_2$-H_2O-UV	96.76 ±0.10	0.18 ±0.02	2.50 ±0.04	85.81 ±0.48	2.50 ±0.04	−0.26 ±0.10	−0.03 ±0.02	0.09 ±0.04	0.09 ±0.04	0.28 ±0.10

Table 6
Lightness (L*), a* and b* parameters, chroma (C*, relative saturation), and h* (hue angle) for pigments, blank paint dosimeters, and outdoor-exposed dosimeters at the Alhambra (A) and the city center of Granada (CC) for 6, 12, 24 months.

	L*	a*	b*	h*	C*	ΔL	Δa	Δb	ΔC	ΔE
Cal-EF	95.35	0.08	1.35	86.64	1.35					
	±0.11	±0.00	±0.02	±0.13	±0.02					
Cal-EF-RG	90.20	−0.39	3.34	96.72	3.36					
	±0.41	±0.02	±0.12	±0.61	±0.11					
Cal-EF-RG-A6	90.22	−0.23	3.61	93.66	3.62	0.02	0.16	0.28	0.26	0.33
	±0.08	±0.04	±0.12	±0.65	±0.12	±0.08	±0.04	±0.12	±0.12	±0.12
Cal-EF-RG-A12	89.68	−0.34	4.15	94.69	4.16	−0.52	0.05	0.81	0.80	0.98
	±0.15	±0.04	±0.18	±0.72	±0.18	±0.15	±0.04	±0.18	±0.18	±0.15
Cal-EF-RG-A24	88.70	−0.23	5.00	92.64	5.00	−1.50	0.17	1.66	1.64	2.26
	±0.44	±0.06	±0.37	±0.90	±0.37	±0.44	±0.06	±0.37	±0.37	±0.52
Cal-EF-RG-CC12	89.58	0.13	2.84	87.47	2.84	−0.62	0.52	−0.50	−0.52	0.98
	±0.22	±0.05	±0.25	±0.81	±0.25	±0.22	±0.05	±0.25	±0.25	±0.21
Cal-EF-RG-CC24	90.76	0.15	2.19	86.09	2.20	0.55	0.54	−1.14	−1.16	1.49
	±0.61	±0.03	±0.17	±0.58	±0.17	±0.61	±0.03	±0.17	±0.17	±0.26
BSG-ST	99.07	0.05	0.80	86.60	0.80					
	±0.01	±0.00	±0.01	±0.17	±0.01					
BSG-ST-RG	96.05	−0.64	4.57	97.97	4.61					
	±0.08	±0.02	±0.11	±0.39	±0.11					
BSG-ST-RG-A6	96.15	−0.19	4.03	92.70	4.04	0.10	0.45	−0.54	−0.58	0.73
	±0.12	±0.03	±0.14	±0.53	±0.14	±0.12	±0.03	±0.14	±0.14	±0.10
BSG-ST-RG-A12	95.12	−0.50	5.83	94.88	5.85	−0.92	0.14	1.26	1.23	1.57
	±0.16	±0.05	±0.11	±0.60	±0.11	±0.16	±0.05	±0.11	±0.11	±0.12
BSG-ST-RG-A24	93.27	−0.23	7.32	91.87	7.32	−2.78	0.41	2.74	2.70	3.93
	±0.46	±0.10	±0.37	±0.89	±0.37	±0.46	±0.10	±0.37	±0.37	±0.59
BSG-ST-RG-CC6	93.63	−0.23	4.02	93.33	4.02	−2.41	0.41	−0.56	−0.59	2.52
	±0.16	±0.03	±0.15	±0.52	±0.15	±0.16	±0.03	±0.15	±0.15	±0.15
BSG-ST-RG-CC12	92.51	−0.26	5.39	92.77	5.39	−3.54	0.38	0.82	0.78	3.65
	±0.19	±0.06	±0.09	±0.60	±0.09	±0.19	±0.06	±0.09	±0.09	±0.19
BSG-ST-RG-CC24	89.31	0.50	5.36	84.71	5.38	−6.73	1.14	0.79	0.77	6.88
	±0.65	±0.16	±0.21	±1.51	±0.22	±0.65	±0.16	±0.21	±0.22	±0.68
BSG-C	98.20	−0.06	1.38	92.48	1.38					
	±0.04	±0.00	±0.01	±0.12	±0.01					
BSG-C-RG	92.19	−0.54	6.00	95.21	6.03					
	±1.00	±0.06	±0.48	±0.93	±0.47					
BSG-C-RG-A6	93.66	−0.45	4.66	95.61	4.69	1.47	0.09	−1.34	−1.34	2.02
	±0.27	±0.05	±0.30	±0.94	±0.30	±0.27	±0.05	±0.30	±0.30	±0.26
BSG-C-RG-A12	93.10	−0.38	8.15	92.68	8.16	0.90	0.16	2.15	2.14	2.35
	±0.28	±0.05	±0.19	±0.40	±0.19	±0.28	±0.05	±0.19	±0.19	±0.17
BSG-C-RG-A24	88.99	0.25	10.67	88.67	10.68	−3.20	0.79	4.67	4.65	5.80
	±0.88	±0.13	±0.61	±0.73	±0.61	±0.88	±0.13	±0.61	±0.61	±0.34
BSG-C-RG-CC6	92.86	−0.19	4.77	92.32	4.77	0.67	0.35	−1.23	−1.25	1.48
	±0.31	±0.08	±0.29	±1.09	±0.28	±0.31	±0.08	±0.29	±0.28	±0.29
BSG-C-RG-CC12	89.08	0.12	5.85	88.82	5.86	−3.12	0.66	−0.15	−0.17	3.19
	±0.70	±0.08	±0.17	±0.74	±0.18	±0.70	±0.08	±0.17	±0.18	±0.69
BSG-C-RG-CC24	88.15 ±0.79	0.55 ±0.09	5.91 ±0.16	84.66 ±0.77	5.94 ±0.17	−4.20 ±0.84	1.11 ±0.10	−0.08 ±0.18	−0.08 ±0.19	4.35 ±0.83

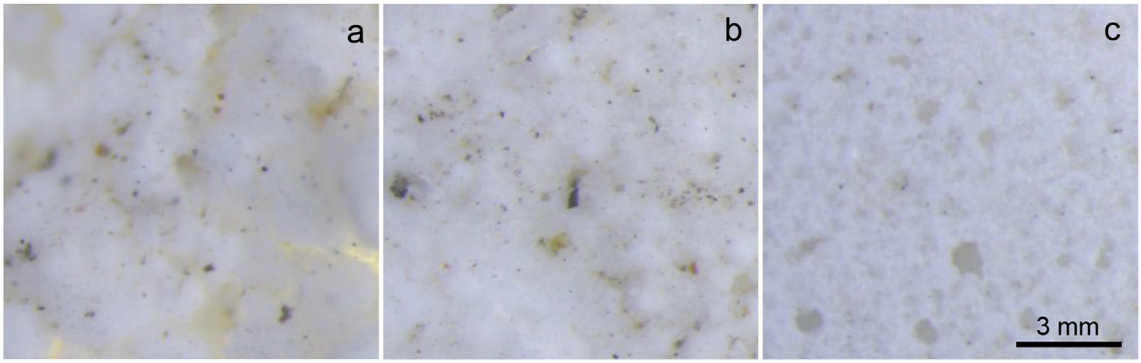

Fig. 13. Microscopic images of (a) BSG-C-based paint; (b) BSG-ST-based paint; and (c) Cal-EF-based paints after 24-month exposure in the city center, showing different degrees of surface soiling.

lightness was affected by particulate matter deposition. Additionally, binder alteration caused a significant increase in b* towards yellow. Yellowing was not observed in samples exposed at the city center, where important binder loss occurred after 6-month of exposure as a result of the direct action of rain and sunlight. Here particulate matter deposition was more severe than at the Alhambra and the primary cause of color change indicated by a progressive decrease in L*. Probably, the rougher surface of BSG-based paints as compared with that of Cal-EF-based paint enabled a better adherence of particle matter and protected the deposited particles from being washed off by rain. Microscopic images corroborate this assumption, showing abundant amounts of dark particulate matter on the surface of BSG-based paints (Fig. 13a and b), whereas paints prepared with Cal-EF (Fig. 13c) hardly suffered any soiling.

4. Concluding remarks

Experimental results showed important mineralogical differences in calcium-based pigments which have significant implications on optical, physical-chemical and mechanical properties as well as on the weathering resistance of the paint films, which may help understand the decay of historical mural paintings and will condition their use in tempera paints for conservation treatments. Generally, the environmental conditions during carbonation greatly influenced the mineralogical evolution of calcium-based pigments as shown by XRD results. From a physical-mechanical point of view fast carbonation and the creation of an interlocked calcite structure as observed in BSG samples (i.e., containing a mixture of portlandite and calcite) exposed in the city center would be preferable. Experimental results have confirmed that carbonation rates were slightly higher in the case of the finer BSG-ST pigment as compared to the coarser BSG-C pigment. The use of finer grained BSG pigments would, thus, be beneficial for obtaining a strong and weather resistant paint film in a shorter period of time.

In dry climates and without the direct action of rain or sunlight, important organic binder degradation is not expected and Cal-EF-based tempera paints (i.e., only containing calcite) can provide adequate weathering resistance. The use of $CaCO_3$-based pigments is especially indicated if mixed with alkaline-sensitive pigments.

In humid climates and/or exposed to the direct action of rain and/or sunlight, in contrast, BSG-based tempera would be preferable as conservation material, which upon carbonation will provide a weather-resistant paint film even after significant organic binder loss has occurred. The incorporation of organics into the newly-formed calcite structure will also improve the paint's chemical and mechanical resistance. Furthermore, the inherent high pH of paints prepared with BSG will confer antibacterial properties to the paint, reducing the risk of organic binder degradation by microorganisms.

In dry climates and under sheltered conditions (i.e., such as the case of samples exposed at the Alhambra), the use of BSG is not required and might even be of disadvantage because metastable calcite precursors or polymorphs can persist. These phases might cause delayed microscopic morphological and volume changes due to phase change even after a prolonged period of time, and do not contribute to an increase in mechanical or weathering resistance of the paint film. Overall, the proteinaceous binder content should be kept to a minimum in order to avoid color changes associated with photo-induced binder degradation.

Experimental results showed that the mineralogical composition of modern, commercially available BSG pigments differed substantially from the reported composition of the historic pigment. Future studies should, thus, address the influence of different $CaCO_3/Ca(OH)_2$ ratios on the morphological evolution as well as on the mechanical and weathering resistance of paint films. Possibly, mixtures of modern BSG pigments and calcite could be used to limit morphological changes but at the same time produce durable, weather-resistant paint films.

Acknowledgements

This research was financed by Spanish Research Projects AER-IMPACT (CGL2012-30729) and EXPOAIR (P12-FQM-1889), the European Regional Development Fund (ERDF), and the Andalusian Research Groups RNM-179. Analyses were performed in the Scientific Instrumentation Center (CIC) of the University of Granada (Spain). J.A. Herrera is funded by a Spanish grant from the AER-IMPACT Project (ref.BES-2013- 065507), and K. Elert is a post-doctoral fellow in the EXPOAIR Project. We thank Carlos Rodriguez-Navarro for comments and suggestions.

References

[1] Schramm HP, Hering B. Historische Malmaterialien und ihre Identifizierung. Verlagsanstalt, Graz: Akademische Druck u; 1988.
[2] Gettens RJ, West Fitzhugh E, Feller RL. Calcium carbonate whites. Stud Conserv 1974;19:157–84.
[3] Kolb U. Electron microscopy on pigments. In: Li ZR, editor. Industrial Applications of electron microscopy. New York: Marcel Dekker Inc.; 2003.
[4] Cennini C. El libro del Arte. Madrid (Spain): AKAL S.L; 1988. p. 264.
[5] Denninger E. What is "Bianco di San Giovanni" of Cennino Cennini? Stud Conserv 1974;19:185–7.
[6] Colalucci G. The frescoes of Michelangelo on the Vault of the Sistine Chapel: original technique and conservation. London July 13-16 1987. In: Cather S, editor. The conservation of wall paintings. Symposium Proceedings. US: J.Paul Getty Trust; 1991. p. 67–76.
[7] Von Endt DW, Baker MT. The chemistry of filled animal glue systems. In:

Bigelow D, editor. Guilded Wood: conservation and history. Madison, Conn: Sound View Press; 1991. p. 155–62.
[8] Colombini MP, Fuoco R, Giacomelli A, Muscatello B. Characterization of proteinaceous binders in wall painting samples by microwave-assisted acid hydrolysis and GC-MS determination of amino acids. Stud Conserv 1998;43:33–41.
[9] Herrera A, Navas N, Cardell C. An evaluation of the impact of urban air pollution on paint dosimeters by tracking changes in the lipid MALDI-TOF mass spectra profile. Talanta 2017;155:53–61.
[10] Ghélis C, Yon J. Protein Folding. New York: Academic Press; 1982.
[11] Merrifield M. Original treatises on the arts of painting, vol. I. New York: Dover Publications Inc.; 1967.
[12] Pacheco F. El arte de la pintura. Madrid: Cátedra; 1990.
[13] www.aemet.es/es/web/serviciosclimaticos/datosclimatologicos/valores climatologicos, [Accessed 18 January 2017].
[14] www.ugr.es/~velilla/meteo-albayzin/resumen.htm, [Accessed 5 April 2017].
[15] www.juntadeandalucia.es/medioambiente/site/rediam/menuitem, [Accessed 27 October 2016].
[16] 2008/50EC. Avance de la evaluación de la calidad del aire en España. Ministerio de Agricultura, Alimentación y Medio Ambiente. Gobierno de España; 2015. p. 41.
[17] Urosevic M, Yebra-Rodríguez A, Sebastián-Pardo E, Cardell C. Black soiling of an architectural limestone during two-year term exposure to urban air in the city of Granada (S Spain). Sci Total Environ 2012;414:564–75.
[18] Martín-Ramos JD. Using XPowder: a software Package for powder x-ray diffraction analysis (GR 1001/04. ISBN 84-609-1497-6). 2004.
[19] Rodriguez-Navarro C, Elert K, Sevcik R. Amorphous and crystalline calcium carbonate phases during carbonation of nanolimes: implications in heritage conservation. Cryst Eng Comm 2016;18:6594–607.
[20] Mokrzycki WS, Tatol M. Colour change ΔE – a survey. Mach Graph Vis 2011;20:383–411.
[21] Fox S, Büsching I, Barklage W, Strasdeit H. Coordination of biologically important α-amino acids to calcium(II) at high pH: insights from crystal structures of calcium α-aminocarboxylates. Inorg Chem 2007;46:818–24.
[22] Das D. Biochemistry. Kolkata (India): Academic Publishers; 2005. p. 885.
[23] Prajapati S, Bhakuni V, Babu KR, Jain SK. Alkaline unfolding and salt-induced folding of bovine liver catalase at high pH. Eur J Biochem 1998;255:178–84.
[24] Kaye GI, Weber PB, Wetzel WM. The alkaline hydrolysis process. 2004.. In: www.alnmag.com/article/2004/alkaline-hydrolysis-process. [Accessed 16 May 2017].
[25] Despotou E, Schlegel T, Shtiza A, Verhelst F. Literature study on the rate and mechanism of carbonation of lime in mortars. Guimaraes, Portugal 7–9 July. In: 9th International Masonry conference 2014. International Masonry Society; 2014. p. 1–12.
[26] Moorehead DR. Cementation by the carbonation of hydrated lime. Cem Concr Res 1986;16:700–8.
[27] Beruto DT, Barberis F, Botter R. Calcium carbonate binding mechanisms in the setting of calcium and calcium-magnesium putty limes. J Cult Herit 2005;6:253–60.
[28] Yang T, Keller B, Gagyari E, Hameter K, Günther D. Direct observation of the carbonation process on the surface of calcium hydroxide crystals in hardened cement paste using an Atomic Force Microscope. J Mater Sci 2003;38:1909–16.
[29] Elert K, Rodriguez-Navarro C, Sebastian Pardo E, Hansen E, Cazalla O. Lime mortars for the conservation of historic buildings. Stud Conserv 2002;47:62–75.
[30] Rodriguez-Navarro C, Jimenez-Lopez C, Rodriguez-Navarro A, Gonzalez-Munoz MT, Rodriguez-Gallego M. Bacterially mediated mineralization of vaterite. Geochim Cosmochim Acta 2007;71:1197–213.
[31] Manoli F, Kanakis J, Malkaj P, Dalas E. The effect of aminoacids on the crystal growth of calcium carbonate. J Cryst Growth 2002;236:363–70.
[32] Xie A-J, Shen Y-H, Zhang C-Y, Yuan Z-W, Zhu X-M, Yang Y-M. Crystal growth of calcium carbonate with various morphologies in different amino acid systems. J Cryst Growth 2005;285:436–43.
[33] Rodriguez-Navarro C, Suzuki A, Ruiz-Agudo E. Alcohol dispersions of calcium hydroxide nanoparticles for stone conservation. Langmuir 2013;29:11457–70.
[34] Rodriguez-Navarro C, Ruiz-Agudo E, Ortega Huertas M, Hansen E. Nanostructure and irreversible coloidal behaviour of $Ca(OH)_2$: implications in cultural heritage conservation. Langmuir 2005;21:10948–57.
[35] Rodriguez-Navarro C, Rodriguez-Navarro A, Elert K, Sebastian E. Role of marble microstructure in near-infrared laser-induced damage during laser cleaning. J Appl Phys 2004;95:3350–7.
[36] Meldrum FC, Cölfen H. Controlling mineral morphologies and structures in Biological and Synthetic systems. Chem Rev 2008;108:4332–432.
[37] Rieger J, Frechen T, Cox G, Heckmann W, Schmidt C, Thieme J. Precursor structures in the crystallization/precipitation processes of $CaCO_3$ and control of particle formation by polyelectrolytes. Faraday Discuss 2007;136:265–77.
[38] Cizer Ö Rodriguez-Navarro C, Ruiz-Agudo E, Elsen J, Van Gemert D, Van Balen K. Phase and morphology evolution of calcium carbonate precipitation by carbonation of hydrated lime. J Mater Sci 2012;47:6151–65.
[39] Orme CA, Noy A, Wierzbicki A, McBride MT, Grantham M, Teng HH, et al. Formation of chiral morphologies through selective binding of amino acids to calcite surface steps. Nature 2001;411:775–9.
[40] Albeck S, Aizenberg J, Addadi L, Weiner S. Interaction of various skeletal intracrystalline components with calcite crystals. J Am Chem Soc 1993;115:11691–7.
[41] Cho KR, Kim YY, Yang P, Cai W, Pan H, Kulak AN, et al. Direct observation of mineral–organic composite formation reveals occlusion mechanism. Nat Commun 2016;7:10187.
[42] Gilbert PUPA, Albrecht M, Frazer BH. The organic-mineral Interface in biominerals. Rev Min Geochem 2005;59:157–85.
[43] Jroundi F, Schiro M, Ruiz-Agudo E, Elert K, Martin-Sanchez I, Gonzalez-Munoz MT, et al. Protection and consolidation of stone heritage by self-inoculation with indigenous carbonatogenic bacterial communities. Nat Commun 2017;8:279.
[44] Kong J, Yu S. Fourier Transform infrared spectroscopic analysis of protein secondary structures. Acta Biochim Biophys Sin 2007;39:549–59.
[45] Odlyha M, Theodorakopoulos C, De Groot J, Bozec L, Horton M. Fourier transform infra-red spectroscopy (ATR/FTIR) and scanning probe microscopy of parchment. E-Preserv Sci 2009;6:138–44.
[46] Leo G, Altucci A, Bourgoin-Voillard S, Gravagnuolo AM, Esposito R, Marino G, et al. Ultraviolet laser-induced cross-linking in peptides. Rapid Commun Mass Spectrom 2013;27:1660–8.
[47] Dilley KJ. Loss of tryotophan associated with photo-polymerization and yellowing of proteins exposed to light over 300 nm. Biochem J 1973;133:821–6.
[48] Aizenberg J, Lambert G, Weiner S, Addadi L. Factors involving in the formation of amorphous and crystalline calcium carbonate: a study of an Ascidian skeleton. J Am Chem Soc 2002;124:32–9.
[49] Addadi L, Raz S, Weiner S. Taking advantage of disorder: amorphous calcium carbonate and its role in biomineralization. Adv Mater 2003;15:959–70.
[50] Thiele ES, French RH. Light-scattering properties of representative, morphological rutile titania particles using a finite-element method. J Am Ceram Soc 1998;81:469–79.